



香港城市大學  
City University of Hong Kong

專業 創新 胸懷全球  
Professional · Creative  
For The World

## CityU Scholars

### Influence of three classic chromium-based transitions on the behavior of film/substrate interface in diamond-like carbon films

Yang, Xi; Yu, Xiang; Wang, Yonghui; Shu, Wen; Hua, Meng

**Published in:**  
Applied Physics Letters

**Published:** 02/12/2013

**Document Version:**  
Final Published version, also known as Publisher's PDF, Publisher's Final version or Version of Record

**Publication record in CityU Scholars:**  
[Go to record](#)

**Published version (DOI):**  
[10.1063/1.4840115](https://doi.org/10.1063/1.4840115)

**Publication details:**  
Yang, X., Yu, X., Wang, Y., Shu, W., & Hua, M. (2013). Influence of three classic chromium-based transitions on the behavior of film/substrate interface in diamond-like carbon films. *Applied Physics Letters*, 103(23), Article 231607. <https://doi.org/10.1063/1.4840115>

#### **Citing this paper**

Please note that where the full-text provided on CityU Scholars is the Post-print version (also known as Accepted Author Manuscript, Peer-reviewed or Author Final version), it may differ from the Final Published version. When citing, ensure that you check and use the publisher's definitive version for pagination and other details.

#### **General rights**

Copyright for the publications made accessible via the CityU Scholars portal is retained by the author(s) and/or other copyright owners and it is a condition of accessing these publications that users recognise and abide by the legal requirements associated with these rights. Users may not further distribute the material or use it for any profit-making activity or commercial gain.

#### **Publisher permission**

Permission for previously published items are in accordance with publisher's copyright policies sourced from the SHERPA RoMEO database. Links to full text versions (either Published or Post-print) are only available if corresponding publishers allow open access.

#### **Take down policy**

Contact [lbscholars@cityu.edu.hk](mailto:lbscholars@cityu.edu.hk) if you believe that this document breaches copyright and provide us with details. We will remove access to the work immediately and investigate your claim.

# Influence of three classic chromium-based transitions on the behavior of film/substrate interface in diamond-like carbon films

Cite as: Appl. Phys. Lett. **103**, 231607 (2013); <https://doi.org/10.1063/1.4840115>

Submitted: 25 August 2013 • Accepted: 19 November 2013 • Published Online: 06 December 2013

Xi Yang, Xiang Yu, Yonghui Wang, et al.



View Online



Export Citation



CrossMark

## ARTICLES YOU MAY BE INTERESTED IN

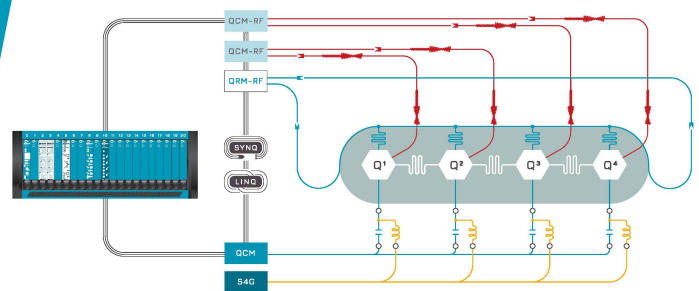
Stress reduction dependent on incident angles of carbon ions in ultrathin tetrahedral amorphous carbon films

Applied Physics Letters **104**, 141908 (2014); <https://doi.org/10.1063/1.4870968>



Integrates all Instrumentation + Software for Control and Readout of **Superconducting Qubits**

visit our website >



## Influence of three classic chromium-based transitions on the behavior of film/substrate interface in diamond-like carbon films

Xi Yang,<sup>1</sup> Xiang Yu,<sup>1,a)</sup> Yonghui Wang,<sup>1</sup> Wen Shu,<sup>1</sup> and Meng Hua<sup>2</sup>

<sup>1</sup>*School of Engineering and Technology, China University of Geosciences (Beijing), Beijing 100083, China*

<sup>2</sup>*MBE Department, City University of Hong Kong, Hong Kong, China*

(Received 25 August 2013; accepted 19 November 2013; published online 6 December 2013)

Three diamond-like carbon (DLC) films with classic chromium-based transitions containing a typical step-like gradient, a linear gradient and a modulation period, were deposited using a mid-frequency dual-magnetron sputtering system. Studies were performed on samples with almost the same Cr content to compare the interfacial structures and compositions of the three chromium-based transitions, and to investigate the internal stress, adhesion strength, and fracture toughness of the films. The synergistic effect of the transitions deterministically influenced the interfacial properties. The films with a linear gradient had the optimal interfacial properties when compared with the other two films. © 2013 AIP Publishing LLC. [<http://dx.doi.org/10.1063/1.4840115>]

Diamond-like carbon (DLC) films have drawn intensive interest because of their properties including their hardness and low friction coefficient.<sup>1</sup> However, the major drawback of DLC films is the tendency for them to accumulate high internal stresses, which is normally induced during the formation of  $sp^3$ -C bonds and readily results in delamination of the films.<sup>2</sup> Hence, approaches in improving the properties of the film/substrate interface to effectively control the internal stress is a hot research topic. The two typical methods are: (i) synthesizing metal-containing DLC films by doping them with metals such as Si, W or Cr to reduce the intrinsic stress and to optimize the stress distribution, but this can cause the hardness of the films to drop irreversibly.<sup>3-5</sup> (ii) Fabricating multilayered films with different alternating functional layers. Interlayers such as Ti and Cr can be adopted to relieve the thermal stress generated by mismatches in the thermal expansion coefficients between the DLC film and the substrate.<sup>6,7</sup> Buffer-layers such as TiN and SiC can be synthesized to improve the load carrying capacity of the films, although this tends to halt the possible elimination of intrinsic stress in the films.<sup>8,9</sup>

These two methods can be effectively used to adjust the internal stress between the layers and to enhance the film/substrate interfacial properties, typically increasing the adhesion performance of the DLC films. Unfortunately, these approaches do not shed any light on the nature of the film performance. Comparisons of the interfacial structures in the films synthesized using different methods gave information on the structure of the interface and the adhesive performance. Each film plays an independent role in correlating the interfaces between two neighboring (top and bottom) layers to bridge/moderate the large differences in the physical properties for better adhesion. Hence, the key to improve the properties of the films is to achieve the synergistic effect between the two layers, bridging them through an appropriate interface transition. Characterization to understand how the interface facilitates enhancement of the mechanism for

the interfacial properties was achieved by synthesizing an integrative film to meet its functional purpose. Two fundamental aspects for the characterization of the interfacial properties are required. They are: the structure and composition of the interface and the internal stress, adhesion strength and fracture toughness of the film.

We deposited three DLC films containing the classic chromium-based transitions (a step-like gradient, a linear gradient and a Cr-modulation period) using a mid-frequency dual-magnetron sputtering system. The interfacial structures and the three chromium-based transitions were compared when the majority of the deposited films had the same Cr content. The investigations aimed to understand the influence of the three Cr-transitions on the properties of the film/substrate interface, and to reveal the mechanism that affected the interfacial properties.

The DLC films with three transitional modes were deposited on substrates of Si (100) wafers for structural analysis and polished H13 stainless steel coupons for behavioral analysis. According to our previous experience in using the mid-frequency dual-magnetron sputtering system,<sup>10</sup> the Cr content of the three transitional modes in the deposited DLC films should be approximately the same. Table I lists the main characteristics and interfacial properties. To make a step-like gradient, the C target current was set to 12 A and the current of the Cr target was controlled according to the modulation frequency, decreasing from 12 A to 2 A within a preset time frame. For a linear gradient, the current of the C target was set to 12 A and the current of the Cr target was controlled according to the modulation frequency, decreasing from 16 A to 1 A within a time frame. For the modulation period, the current for the C and Cr targets were both set to 10 A. The alternating deposition of the Cr target and the DLC film was achieved by controlling the C and Cr target current switches with a Cr: DLC modulation ratio of 1:3.

The elemental compositions across the thickness of the films were measured with auger electron spectroscopy (AES). The valence characteristics of the bond structure in the amorphous carbon network were analyzed using Raman spectroscopy. A scratch tester was used to evaluate the film

<sup>a)</sup> Author to whom correspondence should be addressed. Electronic mail: [yuxiang690625@aliyun.com](mailto:yuxiang690625@aliyun.com). Tel.: +86-10-82320255.

TABLE I. Characteristics and main interfacial properties of the samples.

Transitional mode	Number	Characteristic parameter	Compression stress (GPa)	Critical load (N)	Fracture toughness (MPa $\times$ m <sup>1/2</sup> )	Thickness ( $\mu$ m)
Step-like gradient		Modulation frequency (min)				
	A1	2	2.2	70	2.85	0.6
	A2	4	2.0	76	2.70	0.6
	A3	6	1.9	78	2.65	0.6
Linear gradient		Modulation frequency (s)				
	B1	10	1.8	82	2.62	0.6
	B2	20	1.5	86	2.57	0.6
	B3	30	1.3	90	2.50	0.6
Modulation period		Modulation period ( $\mu$ m)				
	C1	0.2	2.8	65	3.75	1.2
	C2	0.4	2.3	74	2.95	1.2
	C3	0.6	2.5	68	3.28	1.2

adhesion. The internal stress of the films was calculated using the Stoney equation.<sup>11</sup> The fracture toughness was evaluated using data from the measured radial cracks, and was calculated via Eq. (1)<sup>12</sup>

$$K_{IC} = \alpha \left( \frac{E}{H} \right)^{1/2} \times \frac{P}{c^{3/2}}, \quad (1)$$

where  $H$  is the Vickers hardness,  $E$  is the elasticity modulus,  $P$  is the peak load at indentation,  $c$  is the crack length, and  $\alpha$  is an empirical constant that varies with the geometry of the indenter ( $\alpha = 0.016$  for the Vickers indenter).

Changes in the patterns of the multilayered structures were detected and identified with AES measurements. Fig. 1 illustrates in-depth AES patterns of the three Cr-DLC films, where the DLC and Cr layers were identified by the compositions of C and Cr, respectively. Traces of O were negligible. The interface between the graded films and the Si substrate showed an abrupt increase in the amount of Si. Figs. 1(a) and 1(b) shows the atomic fraction of C in the step-like gradient and the linear gradient, which had a consistent decreasing trend starting from a maximum at the outermost film. Simultaneously, the atomic fraction of Cr rose from its minimum value. Formation of the Cr interlayer took place between the DLC film and the substrate, where the largest atomic fraction of Cr was observed. The two structures that varied the interfacial properties were: a change in the composition of the linear gradient usually displayed a

linearly gradient characteristic, and the composition distribution in the step-like gradient generally exhibited a step-change mode with small abrupt increments. Fig. 1(c) illustrates the periodic distribution of the alternating C and Cr peaks in the multilayered phases that were deposited using a modulation period deposition process. The characteristics of the AES spectra in Fig. 1(c) suggest that the graded films on the Si substrates had a DLC/Cr/DLC/Cr structure and the modulation ratios of the C: Cr layers were  $\sim 3:1$ .

Raman spectroscopy is an effective method to analyze the structure of C-C bonds in DLC films.<sup>2</sup> The variation in the  $I_D/I_G$  ratios for the individually synthesized samples is shown as Curve I in Fig. 2. The maximum value of the  $I_D/I_G$  ratio was observed for the films synthesized with the linear gradient deposition process (B1-3), while the samples with a step-like gradient deposition process (A1-3) were lower and the samples with a modulation period deposition process (C1-3) had the lowest ratio. An increase in the  $I_D/I_G$  ratio for the DLC films generally meant that there were less  $sp^3$  bonds and more  $sp^2$  bonds. This implied that the  $sp^3$  content in the B1-3 samples had the lowest  $sp^3$  content, followed by the A1-3 samples, and the C1-3 samples had the highest  $sp^3$  content. It is suggested that the atoms in the transitional metal acted as catalysts for the formation of the  $sp^2$  sites in the amorphous carbon matrix, which subsequently decreased the  $sp^3$  content and increased the  $sp^2$  content.<sup>13</sup> Consequently, samples fabricated using the modulation period deposition process had the lowest  $sp^2$  content and the highest  $sp^3$

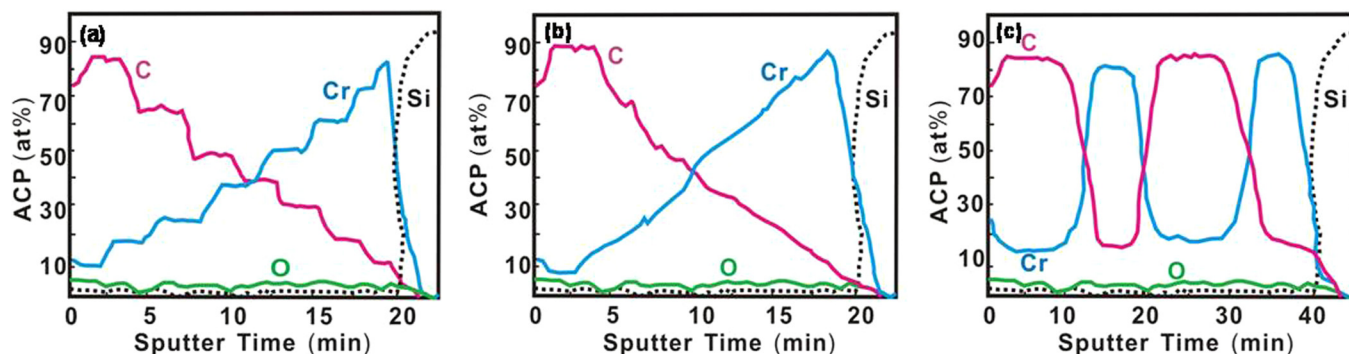


FIG. 1. Elemental concentrations obtained from the AES depth profiles of the three samples. (a) The step-like gradient (A3), (b) the linear gradient (B3), and (c) the modulation period (C2).

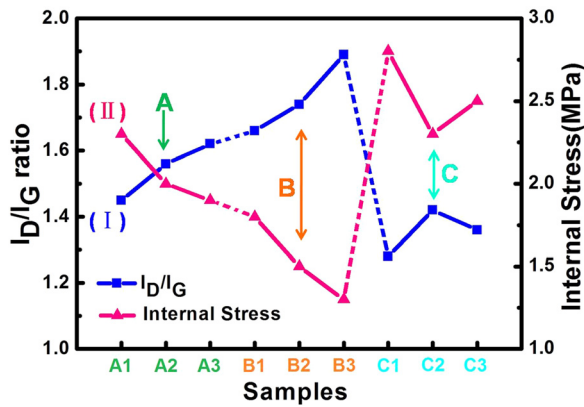


FIG. 2.  $I_D/I_G$  ratio and compressive stress of the samples, where A1-3 are the step-like gradients, B1-3 are the linear gradients, and C1-3 are the modulation periods.

content when compared with the other two counterparts. The mechanism causing the lowest  $sp^3$  content with the linear gradient may be caused by changes in the Cr composition gradient, resulting from the deposition process.

Curve II in Fig. 2 shows the variations in the internal stress for different test samples. This curve indicates that a minimum value of the internal stress for B1-3, A1-3, and C1-3 increased recursively. The leading reason for the internal stress reduction was the decrease in the intrinsic stress in the Cr-DLC film by doping it with Cr. From the Raman analyses, it was concluded that Cr-doping resulted in a decrease in the  $sp^3$  content and an increase in the  $sp^2$  content for the Cr-doped DLC films. According to the results reported by Tay *et al.*,<sup>14</sup> the atomic volume of a  $sp^2$  site is larger than that of a  $sp^3$  site but its in-plane size is smaller because of its shorter bond length. Thus, the formation of  $sp^2$  sites with their  $\sigma$  planes aligned in the plane of the compression relieved the biaxial intrinsic stresses. Moreover, as the doped Cr atoms readily bond with C atoms to form the CrC phase, the formation of the CrC phase reduced the co-ordination numbers of C in the network because C bonded to the carbide in the films. This resulted in a decrease in the local C density and part of intrinsic stress in the DLC film was released. To sum up, among the three transitional modes, the linear gradient (B1-3) had the lowest internal stress, which was mainly attributed to the Cr-doping.

From Table I, the critical load ( $L_c$ ) for nine samples ranged from 65 N to 90 N, where the optimal sample had a

linear gradient. Optical micrographs on the failure regions in the scratch tracks in the DLC films for the three modes are shown in Fig. 3. Traces of peeling along the scratch tracks are shown in Fig. 3(a) for a step-like gradient. The linear gradient shown in Fig. 3(b) only presents an occasional failure of the coating, compared with the step-like gradient, remaining more integral to the film matrix. The modulation period shown in Fig. 3(c) displays delamination of the film. This occurred both inside and outside the scratch track. It was confirmed that the adhesion strength of the linear gradient was higher than the other films.

The enhancement observed in the adhesion strength of the linear and step-like gradients were ascribed to a decrease in the internal stress. The intrinsic stress in the films was decreased by Cr-doping and the extrinsic stress was relieved by inserting a Cr interlayer, which led to a decrease in the thermal stress as a result of the diminishing mismatch in the thermal expansion coefficients. Changes in the microstructure of the interface were also important in improving adhesion.<sup>15</sup> In the step-like gradient there was a small abrupt change in the Cr composition, which formed a micro-interfacial layer and led to accumulation of stress or lattice mismatches between the layers. The linear gradient had a change in the gradient of the Cr composition and a high quality structural continuity to avoid abrupt changes in the performance, improving in the toughness of the interface and modifying the adhesion strength of the films. The linear gradient had the least internal stress and the interfacial structure of the linear gradient followed, thus having the strongest adhesion.

From Table I, the fracture toughness in descending order was: modulation period (C1-3), step like gradient (A1-3) and linear gradient (B1-3). The values of the step-like and linear gradients varied slightly. The fracture toughness refers to the ability of a material to prevent the propagation of cracks and involved many factors. The internal stress played an important role in fracture toughness by acting in the crack propagation direction. The internal stress contains compressive stress and tensile stress, and the compressive stress plays a leading role in hard DLC film. When the cracks propagated, the tensile stress contributed to the crack initiation and growth, and the compressive stress at the crack tip tended to prevent crack propagation. As such, the tensile stress must overcome the compressive stress in the films, consuming any additional energy.<sup>16</sup> Therefore, more compressive stress

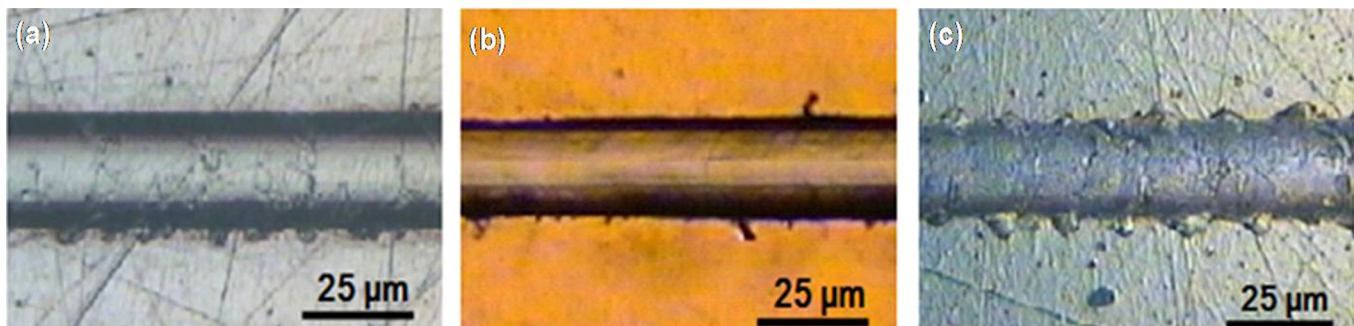


FIG. 3. Optical micrographs of the failure regions on the scratch tracks in the three samples. (a) The step-like gradient A3 ( $L_c = 78$  N), (b) the linear gradient B3 ( $L_c = 90$  N), and (c) the modulation period C2 ( $L_c = 74$  N).

improved the fracture toughness, and the fracture toughness of modulation period is the largest.<sup>17</sup>

The improvement in the fracture toughness was also related to the formation of the multilayered interface.<sup>18</sup> The modulation period of the film was made of alternating Cr and DLC layers. The multilayered structure of the interface could make the crack deflect, effectively preventing plastic deformation. The structure of the multilayered interface also favored higher energy absorption by shear deformation and prevented cracks from propagating during scratch testing. The Cr buffer layer was a soft metal layer. Under the action of a normal load there was a “relative glide” between the hard layers. The soft layers played a role in the shear zone, which prevented the cracks from propagating and improved the fracture toughness of the DLC films. In contrast, the modulation period was the most efficient method.

Fig. 4 shows the mechanism that affected the three interfacial transitions. The major factors affecting the properties of the interface were the Cr interlayer, the Cr buffer layer, CrC, Cr-doping, the  $sp^3$  content, and the interface structures. They each played different roles in either optimization or degradation of the interfacial properties. Therefore, the properties of the interface relied on the synergistic effect. One common characteristic of the three transitional modes was that the Cr interlayers could relieve the

thermal stress generated by the mismatch in the thermal expansion coefficients between the DLC films and the substrates.

For the modulation period, the films were made with alternating deposition of Cr and DLC layers. The soft Cr buffer layer relieved the stresses between the interfaces and slowed down the shock impact from the applied loads. The multilayered interfacial structure prevented crack propagation and effectively prevented plastic deformation, improving the fracture toughness of the DLC films. However, the shortcoming of this transitional mode was that the high intrinsic stress in the DLC films was not resolved. Stress accumulation led to delamination of the films. However, the shortcoming of this transitional mode was that the high intrinsic stress in the DLC films was not resolved. Stress accumulation led to delamination of the films.

The step-like and linear gradients are unique to the Cr-doped DLC films. Thus, both gradients decreased the intrinsic stress in the DLC films by the formation of  $sp^2$  sites and the formation of CrC phase. The  $sp^3$  content in the linear gradient was smaller than the step-like gradient. Thus, the internal stress in the linear gradient was also smaller. In the step-like gradient film, there was a small abrupt change in the Cr composition, a linear gradient was a gradient change that had a continuous structure such

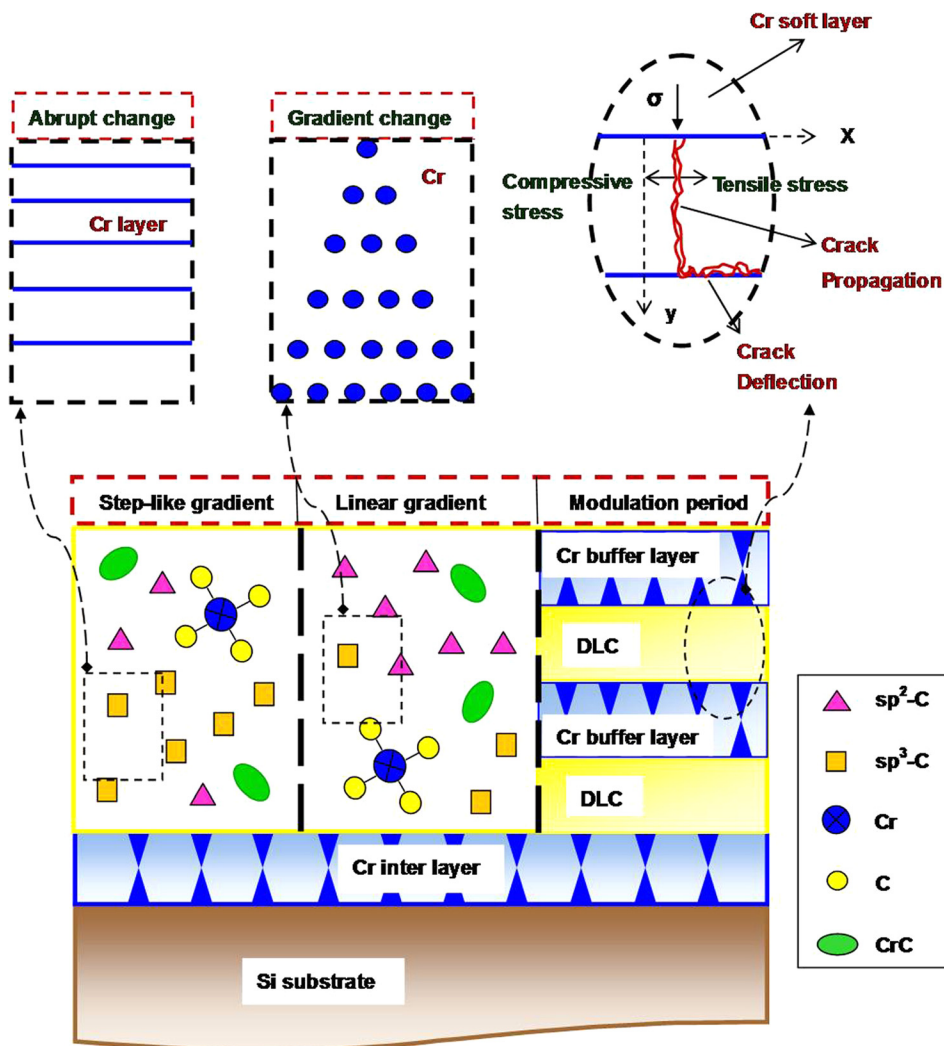


FIG. 4. Mechanism affecting the model of the three interfacial transitions.

that there was not an abrupt change in the performance, leading to the improvement in the adhesion strength of the DLC films. However, due to the low  $sp^3$  content and the different structures, the fracture toughness of the two transitional modes was inferior to the modulation period.

Taking the factors that affect the properties of the interface into account, the linear gradient had the lowest internal stress and the highest adhesion strength. Even when the fracture toughness of the linear gradient was not as good as that of modulation period, the interfacial properties of the DLC films were regarded as the optimal conditions in accordance with the synergistic effect at the interface.

The step-like gradient, linear gradient and the modulation period of the DLC films were prepared using amid-frequency dual-magnetron. When the Cr content was the same in the majority of the films, the influence of the different compositions and structures of the three typical Cr-transitions on the interface properties were investigated. The linear gradient had the least internal stress and the highest adhesion strength. Even though the fracture toughness of the linear gradient was poorer than the modulation period, the properties of the DLC film interface were optimal, according to the synergistic effect of the interface.

This work was supported by (i) National Natural Science Foundation of China under Grant No. 51071143; (ii) the Fundamental Research Funds for the Central Universities under Grant Nos. 2011YXL019 and 2010ZY40; and (iii) a

Foundation for the Author of National Excellent Doctoral Dissertation of PR China under Grant No. FANEDD 201166.

- <sup>1</sup>U. Müller, C. V. Falub, G. Thorwarth, C. Voisard, and R. Hauert, *Acta Mater.* **59**, 1150 (2011).
- <sup>2</sup>G. A. Abbas, S. S. Roy, P. Papakonstantinou, and J. A. McLaughlin, *Carbon* **43**, 303 (2005).
- <sup>3</sup>L. Huang, H. Jiang, J. Zhang, Z. Zhang, and P. Zhang, *Electrochem. Commun.* **8**, 262 (2006).
- <sup>4</sup>V. Singh, V. Palshin, R. C. Tittsworth, and E. I. Meletis, *Carbon* **44**, 1280 (2006).
- <sup>5</sup>Z.-q. Fu, C.-b. Wang, W. Zhang, W. Wang, W. Yue, X. Yu, Z.-j. Peng, S.-s. Lin, and M.-j. Dai, *Mater. Des.* **51**, 775 (2013).
- <sup>6</sup>R. Hauert, C. V. Falub, G. Thorwarth, K. Thorwarth, Ch. Affolter, M. Stiefel, L. E. Podleska, and G. Taeger, *Acta Biomater.* **8**, 3170 (2012).
- <sup>7</sup>C. V. Falub, G. Thorwarth, C. Affolter, U. Müller, C. Voisard, and R. Hauert, *Acta Biomater.* **5**, 3086 (2009).
- <sup>8</sup>Z. Wang and E. Liu, *Talanta* **103**, 47 (2013).
- <sup>9</sup>X. Zhao, X. He, Y. Sun, J. Yi, and P. Xiao, *Acta Mater.* **57**, 893 (2009).
- <sup>10</sup>X. Yu, C. B. Wang, Y. Liu, D. Y. Yu, and Z. Q. Fu, *Surf. Coat. Technol.* **200**, 6765 (2006).
- <sup>11</sup>C. Wang, X. Yu, and M. Hua, *Appl. Surf. Sci.* **256**, 1432 (2009).
- <sup>12</sup>S. Zhang and X. Zhang, *Thin Solid Films* **520**, 2375 (2012).
- <sup>13</sup>M.-W. Huang, J.-Y. Jao, C.-C. Lin, W.-J. Hsieh, Y.-H. Yang, L.-S. Cheng, F. S. Shieu, and H. C. Shih, *Appl. Surf. Sci.* **261**, 21 (2012).
- <sup>14</sup>B. K. Tay, Y. H. Cheng, X. Z. Ding, S. P. Lau, X. Shi, G. F. You, and D. Sheeja, *Diamond Relat. Mater.* **10**, 1082 (2001).
- <sup>15</sup>C. V. Falub, U. Müller, G. Thorwarth, M. Parlinska-Wojtan, C. Voisard, and R. Hauert, *Acta Mater.* **59**, 4678 (2011).
- <sup>16</sup>L. Zhang, H. Yang, X. Pang, K. Gao, and A. A. Volinsky, *Surf. Coat. Technol.* **224**, 124 (2013).
- <sup>17</sup>Y. Zhang, D. Givord, and N. M. Dempsey, *Acta Mater.* **60**, 3783 (2012).
- <sup>18</sup>S. Q. Lu, H. Z. Zheng, and M. W. Fu, *Scr. Mater.* **61**, 206 (2009).